

## THE SPREAD AND VAPORISATION OF CRYOGENIC LIQUIDS ON WATER

P.J. WAITE, R.J. WHITEHOUSE, E.B. WINN

*Cremer and Warner, 140 Buckingham Palace Road, London SW1 (Gt. Britain)*

and W.A. WAKEHAM

*Department of Chemical Engineering and Chemical Technology, Imperial College, London SW7 (Gt. Britain)*

(Received July 12, 1982; accepted in revised form May 31, 1983)

### Summary

The literature on the spread and vaporisation of cryogenic liquids on water is reviewed and a new model proposed. The model incorporates the features of gravity spreading of the liquid pool, mass conservation, heat transfer from the water and the effects of two-component LNG (methane and ethane). The new model is tested against experimental results for LNG and it is found that the heat transfer rates to LNG spreading on unconfined turbulent water are typical of film boiling rates.

---

### Introduction

The spread of a liquid on another liquid of greater density is difficult to describe mathematically. When the spreading liquid is a cryogen such as liquefied natural gas (LNG), the additional complexity of simultaneous heat transfer and vaporisation has rendered a complete description of the process intractable. Furthermore, although there have been a number of attempts to treat individual aspects of the problem, particular areas remain unexplained, notably that of heat transfer to the spreading pool. In view of the importance of the topic in the context of hazard analysis of cryogenic storage and transportation systems, a review of earlier studies has been made to identify those areas requiring most attention. Subsequently a new, more comprehensive study has been carried out and forms the subject of this paper. The study has been performed specifically on LNG, but can be generalized for other cryogenic and similar liquids.

### Review

One of the early treatments of the spread of oil on water was carried out by Fay in Ref. [1] using dimensional analysis arguments and the simple idea that the pool spread is a result of the loss of potential energy of the oil pool. He identified three stages of the evolution of the pool according to the relative importance of the gravitational, inertial, viscous and surface tension forces

to its motion. Fannelop and Waldman in Refs. [2] and [3] used the same ideas to derive analytical results for the pool dimensions as a function of time. In particular, for a radial pool, they found, with their model for the initial phase of the spill in which gravitational forces and inertial forces are significant, that the radius of the pool increased as  $(\text{time})^{1/2}$ . Raj and Kalelkar in Refs. [4] and [5] derived analytical solutions for the spread of a cryogenic liquid on water using Fannelop and Waldman's results [2,3] to obtain boundary conditions for their equations, and assuming either a constant heat flux or a heat flux governed by the presence of an ice layer. No satisfactory justification for either heat transfer model was offered. Other analyses based on Fannelop and Waldman's basic theory and data from experimental LNG spills have also been published (e.g., Gideon et al. [6] and May and Perumal [7]). However, all these models deal more with the mechanics of pool spread rather than heat transfer.

Insofar as heat transfer to a spreading pool is concerned, it is safe to assume that the predominant source of heat is from the water, but the possibilities of ice formation, convective motion in the water and the presence of waves make a description of the process complicated. There is particular confusion in the literature over whether a layer of ice will or will not form. Some heat transfer models assume that ice will form, whereas other models merely assume a constant heat flux, and do not address the mechanism of heat transfer. In general, all earlier attempts to predict vaporisation rates for cryogenic liquids on water have been founded on very simple models of the system and often quantitatively based on experimental observations of the vaporisation rates.

Most experimental work has been carried out in circumstances where the cryogenic liquid is spilled onto a confined water surface. Frequently the cryogen involved has been liquefied natural gas (e.g., [8]) although pure, light hydrocarbons and other liquefied gases have also been used (e.g., [9]). Less often experimental observations have been carried out on unconfined water surfaces [8,10,11]. Even in the case of the confined spillage experiments it has not been possible to determine heat transfer rates directly; rather, they have been inferred from observation of the rate of change of mass of the spilled cryogen (e.g., [9,12]). In unconfined spillages the determination of the heat transfer rate has been even less direct (e.g., [11]). In only a few cases have temperature measurements been performed in the bulk of the supporting water (e.g., [13]). Generally, but not invariably, ice formation has been observed to accompany vaporisation from a confined surface (e.g., [9]), whereas it has seldom been reported in significant quantities on unconfined surfaces. Furthermore, on confined surfaces the heat flux to liquefied natural gas on water reveals a maximum which occurs some 25 seconds after the spillage, whereas in an unconfined test such a peak has not been observed (e.g., [11]).

Given the incomplete experimental information above, it is perhaps not surprising that estimates of the heat flux from water to liquefied gas pools have ranged over a factor of 4, from 25 kW/m<sup>2</sup> to 100 kW/m<sup>2</sup>. Moreover,

because no coherent model exists which provides a complete description of all the available information, it has been usual for workers in the field to choose a single value of the heat flux from the range and to apply this uniformly under any conditions.

Over the last ten years a number of models of increasing sophistication have been proposed for the evaluation of the heat flux to a cryogenic liquid from water. Some models, such as those of Hoult [14] and Fay [15] have been based on the supposition that a coherent ice layer is always formed on the water surface, which grows throughout the vaporisation period. Although Fay's model is the more realistic, since it accounts for the sensible heat loss of the ice as it cools, the experimental evidence for unconfined spills indicates that the formation of ice is not a necessary event, so that neither model is universally applicable. Opschoor [16] distinguished between confined and unconfined spills and formulated different models for the two cases. For the unconfined spill it was assumed that no ice is formed and that the heat is supplied by turbulent natural convection in the water. Turner's analysis of convection across a density interface [17] was then employed to estimate the heat flux to the cryogen and the results were broadly consistent with experimental observations. However, the applicability of the analysis to every case of cryogenic liquids evaporating on water is by no means clear. For confined spills, Opschoor's analysis was restricted to a period of 25 seconds after the initial contact between the cryogen and water which coincided with the experimentally observed maximum in the heat flux. The decrease in the heat flux after this maximum was attributed to the formation and growth of a coherent ice layer and the predictions of the model were in agreement with observation. In a similar paper [18] Opschoor has extended the model to burning pools of LNG.

Valencia-Chavez has conducted a set of carefully controlled experiments with confined spills of cryogens on water [9]. The cryogens studied were light hydrocarbon mixtures of different compositions including some representing typical liquefied natural gases. He observed that the initial heat fluxes for samples also containing ethane and propane were higher than for samples of pure methane and that the maximum in the heat flux occurred at earlier times. In order to explain these observations it was assumed that the cryogen initially vaporises by film boiling and that a thin layer of ice forms at the water surface immediately following the spillage. As time proceeds the ice layer grows and causes a reduction in the heat flux until eventually the vapour film from boiling collapses, transition occurs and nucleate boiling begins on the ice surface. By means of a correlation of the observed times of film collapse and a mathematical model of the heat transfer through the growing ice layer a satisfactory description of the behaviour in the confined spill experiments was obtained.

Despite the development and partial success of some of the foregoing models of heat transfer to boiling cryogens on water surfaces, particularly that of Valencia-Chavez in Ref. [9], there still exists no coherent description

on the process which is generally applicable to all situations. In this paper an attempt is made to produce such a description. It is intended that the model should be as independent as possible of particular empirical observations. Furthermore, it should apply to a wide range of situations encountered in practice, encompassing those created in laboratory experiments which then serve as a test of the model.

There are more models for spread and vaporisation of liquid cryogens than have been mentioned here, see for examples refs. [19–22]. Raj also gives more references in his paper [23].

### Pool spread

Fannelop and Waldman's analysis of oil spread [2,3] resulted in the following dependence of slick radius on time in the "gravity-inertia" phase.

$$R = K \left[ \frac{(\rho_w - \rho_o)}{\rho_w} g L^3 t^2 \right]^{1/4} \quad (1)$$

where  $R$  = slick radius;  $K$  = constant of proportionality (1.14);  $\rho_w$  = density of water;  $\rho_o$  = density of oil,  $g$  = acceleration due to gravity;  $L$  = linear dimension representing size of oil spill; and  $t$  = time.

One boundary condition required to produce the above results is the velocity at the pool edge, which is:

$$U_{LE} = \left[ k_1 \frac{(\rho_w - \rho_o)}{\rho_w} g h_{LE} \right]^{1/2} \quad (2)$$

where  $k_1$  is a constant and  $h_{LE}$  is the thickness of the pool at its leading edge. Fannelop and Waldman assume  $k_1 = 1$ , which is analogous to the characteristic wave speed for a small disturbance. The two constants are related by:

$$K = \left[ \frac{128 k_1}{4\pi(8 - 2k_1)} \right]^{1/4} \quad (3)$$

as shown by Fannelop and Waldman.

The detailed analysis predicts a spreading pool to be thickest at its edge and thinnest at its centre. The relationship between depth,  $h$ , and radius,  $R$ , is:

$$h = \frac{2}{3\pi} \frac{L^3}{R_{LE}^2} \left[ 1 + \left( \frac{R}{R_{LE}} \right)^2 \right] \quad (4)$$

where  $R_{LE}$  is the pool radius at the leading edge. This prediction is in agreement with some observations of LNG spills on water. Burgess et al. [10] reported that a bare patch appeared at the centre of the spills they conducted. However, in recent experiments [24] the liquid pool is described as having approximately constant dimensions.

The Raj and Kalelkar [4, 5] analysis of cryogenic spills is based on the premise that a pool is a perfect cylinder. The spread rate is calculated from a force balance with the loss of potential energy being equated to "inertial resistance". The results of Fannelop and Waldman are used to obtain boundary conditions in the integration of the force balance differential equation. This combination is not valid since the premise of a perfect cylinder and the incorporation of a vaporisation term are inconsistent with Fannelop and Waldman theory.

May and Perumal [7] argue that the Fannelop and Waldman theory is valid for short times, but that the constant of proportionality,  $K$ , might be different. From eqn. (1):

$$\frac{dR}{dt} = \frac{K}{2} \left[ \frac{(\rho_w - \rho_L)}{\rho_w} g L^3 \right]^{1/4} t^{-1/2} \quad (5)$$

where  $\rho_L$  is the density of LNG.

By simulating a series of experimental LNG spills with this equation, they found that  $K = 1.35$  provided good agreement with actual pool spread rates. From eqn. (3), the constant  $k_1$  in eqn. (2) is calculated to be 1.6.

Although an LNG pool is not strictly a perfect cylinder, it clearly approximates to a cylinder. For this reason, and because of the difficulty in deriving an analytical description of an LNG pool, it was decided to assume that a pool can be described as a cylinder which spreads at a rate given by the leading edge velocity (eqn. (2)) with  $k_1 = 1.6$  and  $h_{LE}$  taken to be the average pool thickness,  $h_A$ . The pool mass and geometry are thus described by:

$$\text{geometry:} \quad h_A = \frac{M}{\rho_L \pi R^2} \quad (6)$$

$$\text{mass balance:} \quad M = M_0 + \int \left( \frac{dM_s}{dt} - \frac{dM_v}{dt} \right) dt \quad (7)$$

$$\text{heat balance:} \quad \frac{dM_v}{dt} = \pi R^2 \phi h_{fg} \quad (8)$$

where  $M$  = pool mass;  $M_0$  = initial mass;  $dM_s/dt$  = spill rate;  $dM_v/dt$  = vaporisation rate;  $\phi$  = heat flux to pool; and  $h_{fg}$  = latent heat of vaporisation.

In addition it is assumed that there is a minimum depth for the liquid pool which will limit its spread. This minimum depth is dependent on the surface and for water is taken as 1.8 mm (cf. Ref. [8], where the minimum depth is proportional to (diameter of pool)<sup>0.56</sup> and which gives 15% lower peak vaporisation rates). This model was extended to describe the vaporisation rate of separate LNG components by assuming that the vapour phase is in equilibrium with the liquid phase. This assumption was verified for confined LNG spills on water by Valencia-Chavez.

For simplicity, the LNG was assumed to consist of two components, methane (A) and ethane (B). The overall mass balance on component A is:

$$\frac{d(W_m x_A)}{dt} = L_m x_{AS} - G_m y_A \quad (9)$$

where  $W_m$  is the number of moles of material in the pool,  $L_m$  the molar spill rate,  $G_m$  the molar vaporisation rate;  $x_A$  and  $x_{AS}$  represent the methane proportion of the liquid pool and the spilling liquid respectively;  $y_A$  denotes the methane proportion of vapour. The suffix B is used to denote ethane fractions.

Overall enthalpy balance on the pool:

$$\frac{d(W_m i_p)}{dt} = L_m i_s + \pi R^2 \phi - G_m i_v \quad (10)$$

where  $i$  is enthalpy; suffices  $s$  and  $v$  denote the spilling liquid and the vaporising fractions, respectively.

Composition of the liquid and vapour phases:

$$x_A + x_B = 1 \quad (11)$$

$$y_A + y_B = 1 \quad (12)$$

Phase equilibrium relationships:

$$\frac{y_A}{x_A} = K_A \quad (13)$$

$$\frac{y_B}{x_B} = K_B \quad (14)$$

$K_A$  and  $K_B$  are both functions of pool temperature and composition.

The model assumes for simplicity uniform pool temperature and composition. The model was used as a basis for evaluating the heat transfer model described below.

## Heat transfer

As mentioned in the introduction the complexity of the process of boiling of cryogenic liquids on water renders its complete description intractable. However, there is considerable merit in the development of a representation of the process which, although it does not include every detail, encompasses all of its important features. Such a model is essential for the interpretation of experimental data obtained in the laboratory as well as for their interpolation and extrapolation to large scale spillages.

In order to adhere to this philosophy we first identify the most important

processes in the heat transfer and neglect those of a secondary nature entirely. The discussion in the introduction has indicated that film boiling, nucleate boiling and the transition between them can be important factors in the process, together with turbulent convective mixing in the water and ice formation. It has sometimes been suggested that, in the case of liquefied hydrocarbons, hydrate formation (Opschoor [16]), water entrainment (Boyle and Kneebone [11]) and waves on the water surface may be significant, but in our analysis these are assumed to be secondary processes and are neglected entirely.

### Initial heat transfer process

For the purpose of this analysis the cryogen is supposed to take the form of a flat cylinder of uniform temperature and composition, above the water surface. If the spill is unconfined then the radius of the cylinder,  $R^*(t)$ , increases with time as described above. At time  $t = 0$  it is assumed that the

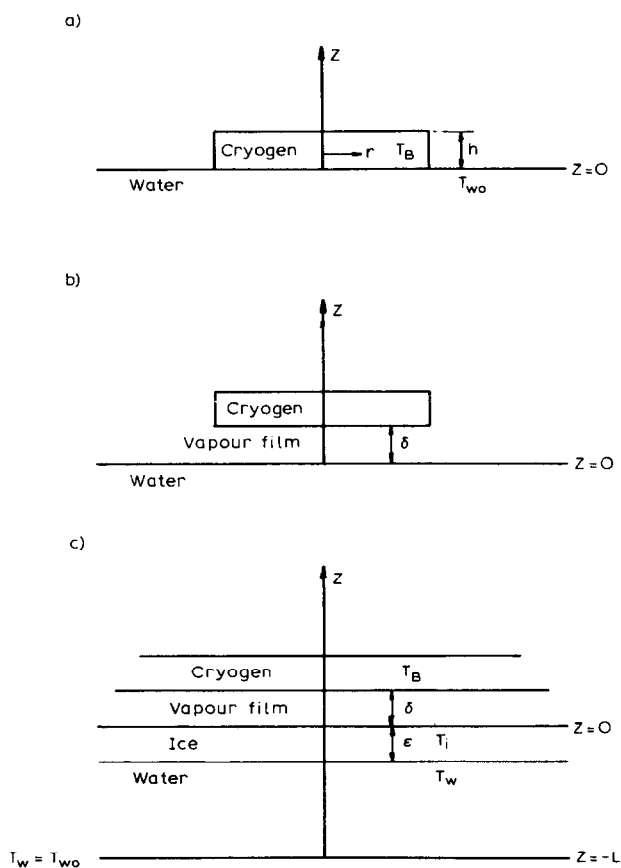


Fig. 1. Diagrams of models of heat transfer to cryogenic liquids boiling on water ; (a) the situation near  $t = 0$  at the start of the boil-off; (b) the situation during film boiling on water; (c) boiling during ice formation.

cryogenic fluid is in direct contact with the water but does not intrude below the water surface, as indicated in Fig. 1a. In this figure  $T_B$  is the temperature of the cryogen (its boiling point) and this may be a function of time if the cryogen is a mixture of components of different relative volatilities. If it is assumed the mechanism of heat transfer may be represented by a conduction equation, then the heat flux to the LNG may be obtained from the solution to the three-dimensional Fourier equation:

$$\frac{\partial^2 T_w}{\partial z^2} + \frac{1}{r} \frac{\partial}{\partial r} \left( r \frac{\partial T_w}{\partial r} \right) = \frac{\rho_w C_{pw}}{\lambda_w} \frac{\partial T_w}{\partial t} \quad (15)$$

subject to the boundary conditions

$$0 \leq r \leq R^*(t), \quad z = 0, \quad t > 0, \quad T_w = T_B$$

(This is actually the boundary condition at the boundary of the vapour film and liquid cryogen but the vapour film is neglected at this stage; also the formation of ice is discussed later.)

$$\begin{aligned} r > R^*(t), \quad z = 0, \quad t > 0, \quad T_w = T_{w0} \\ \text{for all } r \text{ and } t, \quad z = -\infty, \quad T_w = T_{w0} \\ \text{and for all } r \text{ and all } z, \quad t < 0, \quad T_w = T_{w0} \end{aligned} \quad (16)$$

where  $R^*(t)$  is the radius of the LNG pool at a particular instant.

In these equations  $T_w$  is the water temperature at time  $t$  and  $T_{w0}$  its value at times  $t \leq 0$ . The quantities  $\lambda_w$ ,  $\rho_w$  and  $C_{pw}$  represent respectively the effective thermal conductivity, density and heat capacity of the water. Although an analytic solution to eqn. (15) subject to these conditions is possible, a simpler and sufficiently accurate solution may be obtained by deriving the spatial variation of the temperature in the water from the solution to the three-dimensional problem in steady state, and the time dependence of the temperature from the transient one-dimensional case. That is to say the spatial variation of temperature is obtained from the solution of the equation:

$$\frac{\partial^2 T_w}{\partial z^2} + \frac{1}{r} \frac{\partial}{\partial r} \left( r \frac{\partial T_w}{\partial r} \right) = 0 \quad (17)$$

with boundary conditions

$$\begin{aligned} 0 < r < R^*, \quad z = 0, \quad T_w = T_B \\ \text{for all } r, \quad z = -\infty, \quad T_w = T_{w0} \end{aligned} \quad (18)$$

whereas the temporal variation of the temperature is obtained from the solution of the equation:

$$\frac{\partial^2 T_w}{\partial z^2} = \frac{\rho_w C_{pw}}{\lambda_w} \frac{\partial T_w}{\partial t} \quad (19)$$

with boundary conditions

$$\begin{aligned} \text{for all } z, \quad t \leq 0, \quad T_w &= T_{w0} \\ \text{for } z = 0, \quad t > 0, \quad T_w &= T_B \\ \text{and } z = -\infty \text{ for all } t, \quad T_w &= T_0 \end{aligned} \quad (20)$$

Both equations have standard solutions (Carslaw and Jaeger [25]) which may be combined in a way which satisfies all boundary conditions to yield for the temperature of the water

$$T_w(r, z, t) = T_{w0} - (T_{w0} - T_B) \operatorname{erfc} \left( \frac{-z}{2\sqrt{k_w t}} \right) \frac{2}{\pi} \sin^{-1} \left\{ \frac{2R^*}{[(r-R^*)^2 + z^2]^{1/2} + [(r+R^*)^2 + z^2]^{1/2}} \right\} \quad (21)$$

in which  $k_w$  is the thermal diffusivity of the water. The physical meaning of the approximations involved in this solution is that the three-dimensionality of the heat transfer process represents only a first-order perturbation to the one-dimensional case which, for pools of large diameter relative to the thermal boundary layer in the water, is likely to be the case. The heat flux to the cryogenic fluid,  $q$ , is then simply calculated according to the equation:

$$q = -\lambda_w \left( \frac{\partial T_w}{\partial z} \right) \Big|_{z=0} \quad (22)$$

to yield

$$q = \lambda_w (T_{w0} - T_B) \left[ \frac{1}{(\pi k_w t)^{1/2}} + \frac{2}{\pi (R^{*2} - r^2)^{1/2}} \right] \quad (23)$$

Equation (23) represents the heat flux on the assumption of contact between the cryogen and the water, but if this value exceeds some critical value stable film boiling will result, leading to a different process for heat transfer. Stermann [26], Kutateladze [27] and Moissis and Berenson [28] have given expressions for the minimum heat flux,  $q_{\text{crit}}$ , necessary to sustain stable film boiling. They read:

$$q_{\text{crit},1} = 0.168 h_{1v} \rho_v^{1/2} [g \sigma_1 (\rho_1 - \rho_v)]^{1/4} \quad (24)$$

and

$$q_{\text{crit},2} = \frac{0.18 \rho_v h_{1v} [(\rho_1 - \rho_v) / \rho_1 \rho_v]^{1/2} [g \sigma_1 (\rho_1 - \rho_v)]^{1/4}}{1 + 2(\rho_v / \rho_1)^{1/2} + (\rho_v / \rho_1)} \quad (25)$$

where  $h_{1v}$  is the latent heat of vaporisation for the cryogen and subscripts l and v indicate liquid and vapour, respectively. For our model it is supposed that stable film boiling will occur if:

$$q > q_{\text{crit},1} \text{ and } q > q_{\text{crit},2}. \quad (26)$$

As an example, for a typical liquefied natural gas pool the initial heat flux,  $q$ , is about  $1.5 \text{ MW/m}^2$ , whereas the critical heat fluxes are of the order of  $0.3 \text{ MW/m}^2$ . Thus we conclude that the initial phase of any vaporisation process of LNG on water takes place through film boiling, which is consistent with the observations of Valencia-Chavez [9].

### Film boiling model

In the previous section the conditions under which stable film boiling will occur have been established. When film boiling occurs the physical model of the system becomes that of Fig. 1b, in which the cryogen at its boiling point is separated from the water surface by a layer of vapour thickness  $\delta$ .

In this case we can again describe the problem by means of Fourier's conduction equation although it should not necessarily be assumed that the conductivity in a particular phase is identical to the molecular conductivity, because it may be augmented by convective motion, which was not considered in the previous section.

The two equations for the vapour film and the water are:

$$\frac{\partial T_v}{\partial t} = \frac{\lambda_v}{\rho_v C_{pv}} \frac{\partial^2 T_v}{\partial z^2} \quad 0 < z < \delta, \quad t > 0 \quad (27)$$

and

$$\frac{\partial T_w}{\partial t} = \frac{\lambda_w}{\rho_w C_{pw}} \frac{\partial^2 T_w}{\partial z^2} \quad z < 0, \quad t > 0 \quad (28)$$

with boundary conditions

$$\begin{aligned} z = 0, \quad t > 0, \quad \lambda_v \partial T_v / \partial z &= \lambda_w \partial T_w / \partial z \\ z = 0, \quad t > 0, \quad T_v &= T_w \\ z = \delta, \quad t > 0, \quad T_v &= T_B \\ 0 \leq z < \delta, \quad t < 0, \quad T_v &= T_w = T_{w0} \\ z \rightarrow -\infty, \quad \text{all } t, \quad T_w &= T_{w0} \end{aligned} \quad (29)$$

The penultimate condition of this set implies the assumption that the vapour film is initially at the bulk water temperature. Although not exact, the quantitative consequences of this assumption are expected to be small, and as far as the water is concerned this is of much smaller consequence than the boundary conditions (16) above.

The values to be employed for the thermal conductivities of the vapour and water are not certain since there may be convective contributions to the apparent values of both. We therefore adopt the approach that these quantities may be empirical parameters of the model for a particular case. It is

interesting to note here that there may be significant differences in the appropriate thermal conductivities between spills on fresh water and sea water because the former displays a maximum density at 4°C which provides a stable density stratification whereas the latter does not.

In the case when the film thickness,  $\delta$ , is small, eqns. (27) and (28) are readily solved using Laplace transforms to yield the temperature profile in the water and the associated heat flux [18]. The results are:

$$T_w = T_{w0} + (T_B - T_{w0}) \left\{ \operatorname{erfc} \left( \frac{-z}{2\sqrt{k_w t}} \right) - \exp \left[ \left( \frac{\lambda_v}{\lambda_w} \right) \frac{z}{\delta} + \frac{k_w t}{\delta^2} \left( \frac{\lambda_v}{\lambda_w} \right)^2 \right] \right. \\ \left. \times \operatorname{erfc} \left[ \frac{-z}{2\sqrt{k_w t}} + \left( \frac{\lambda_v}{\lambda_w \delta} \right) \sqrt{k_w t} \right] \right\} \quad (30)$$

with

$$q_{\text{film}} = -\lambda_w \left( \frac{\partial T_w}{\partial z} \right) \Big|_{z=0} \quad (31)$$

The film thickness,  $\delta$ , may itself be obtained from an empirical correlation given by Hsu and Graham [29]:

$$\delta = (2.6-1.9) \left[ \frac{\mu_v \lambda_v \Delta T}{h_{1v} \rho_v g (\rho_1 - \rho_v)} \sqrt{\frac{\sigma_1}{g (\rho_1 - \rho_v)}} \right]^{1/4} \quad (32)$$

which presumes a laminar vapour layer. In this equation  $\mu_v$  is the viscosity of the vapour,  $\Delta T$  the temperature difference across it and  $\sigma_1$  the surface tension of the liquid. If a mean value of the numerical coefficient is employed the film thickness for liquefied natural gas boiling on water is  $10^{-4}$  m, which is consistent with a value reported by Boyle and Kneebone [11].

### *The transition to nucleate boiling*

There are two possible mechanisms whereby the film boiling process described in the previous section may be transformed to nucleate boiling. First the cooling of the water surface may eventually lead to ice formation, thereby reducing the temperature difference and promoting film collapse. Secondly, in boiling of mixtures of cryogenic liquids, the preferential vaporisation of the more volatile component [11] leads to an increasing temperature of the boiling liquid and hence a reduction of the heat flux. In the most general case both mechanisms can occur.

In any event the transition to nucleate boiling may be characterized by a critical heat flux,  $q_{\text{Leid}}$ , which corresponds to the Leidenfrost point. Zuber [31] has given the correlation:

$$q_{\text{Leid}} = \frac{\pi}{24} \frac{h_{1v} \rho_v}{(\rho_1 + \rho_v)^{1/2}} [\sigma_1 g (\rho_1 - \rho_v)]^{1/4} \quad (33)$$

for this critical heat flux. It could be presumed in the model that whenever the heat flux computed from eqns. (30)–(32) falls below this value, for whatever reason, that is,

$$q_{\text{film}} < q_{\text{Leid}}, \quad (34)$$

then nucleate boiling occurs. This is provided that the process of film boiling occurred initially, based on the conditions given by Ref. [26].

An alternative, heuristic approach to the problem of film collapse is provided by the work of Valencia-Chavez [9], for cases of confined spills when ice is formed during the boiling of light hydrocarbon mixtures. Valencia-Chavez [9] observed the time at which the vaporisation rate attained its maximum and identified this as the time of film collapse,  $t_{fc}$ . This is also the time when ice forms. If this approach is adopted then a second criterion for the transition to nucleate boiling is:

$$T_w(z = 0) < T_F \quad (35)$$

where  $T_F$  is the freezing point of water.

In the absence of any better guidance it has been presumed in general that the transition occurs when either condition (34) or condition (35) is satisfied. In the case that no ice is formed, the heat flux could be computed from the equations (15)–(23) but if ice forms a new analysis is necessary. In the next section such an analysis is described.

### *Boiling on ice*

When ice is formed on the water surface the heat for the vaporisation is provided by the latent heat of fusion of the ice and the subsequent cooling, thus a new set of equations are required to describe the process. In general, the ice will float on the water surface, protruding only slightly above it. However, for simplicity, and because the error introduced is small it is presumed that the ice layer floats on top of the water surface, as shown in Fig. 1c. This is equivalent to the neglect of edge effects. In general, the ice may be separated from the cryogen by a vapour film as shown in Fig. 1c, although this will evidently not be the case if criterion (35) is used for film collapse. In either event, as will be seen, the basic analysis remains unchanged by virtue of the choice of boundary conditions for the problem. Denoting by  $\theta$  temperatures with respect to the freezing point of water,  $T_f$ , so that:

$$\theta = T - T_F \quad (36)$$

and employing the subscript *i* to indicate the ice, the equations governing the temperature in the ice–water system may be written:

$$\frac{\partial \theta_i}{\partial t} = k_i \frac{\partial^2 \theta_i}{\partial z^2} \quad (37)$$

in the ice and

$$\frac{\partial \theta_w}{\partial t} = k_w \frac{\partial^2 \theta_w}{\partial z^2} \quad (38)$$

in the water. The coupling equation between the two regions is

$$\frac{d\epsilon}{dt} = -\frac{1}{\rho_w L_{wi}} \left[ \lambda_i \left( \frac{\partial \theta_i}{\partial z} \right)_{z=-\epsilon} - \lambda_w \left( \frac{\partial \theta_w}{\partial z} \right)_{z=-\epsilon} \right] \quad (39)$$

where  $\epsilon$  is the depth of the ice layer and  $L_{wi}$  is the latent heat of fusion of water. If it is supposed that the surface of water attains the freezing temperature at a time  $t_1$  after the initiation of the spill then the initial condition for the solution of equations (37)–(39) is:

$$\text{at } t = t_1, \quad \theta_w(t_1, z) = T_w(t_1, z) - T_F \quad \text{for all } z \quad (40)$$

where  $T_w(t_1, z)$  is the temperature profile calculated with the aid of the preceding analysis. The two spatial boundary conditions which must be specified concern conditions at the ice surface and the temperature of the water at an infinite depth.

For the former we have adopted the best available condition proposed by Valencia-Chavez [9]

$$\theta_i(z=0) = (t/t_{fc}) (T_{B(t)} - T_f) \quad t < t_{fc}$$

and (41)

$$\theta_i(z=0) = (T_{B(t)} - T_f) \quad t > t_{fc}$$

according to whether film boiling persists or not judged on the criteria of either equation (33) or (26). The time for film collapse,  $t_{fc}$ , is dependent on hydrocarbon composition. Correlations proposed by Valencia-Chavez are used to calculate this parameter. Because equations (37)–(39) cannot be solved analytically the second condition is not established at  $z = -\infty$ , but rather at  $z = -l$ , where  $l$  is a depth in the water chosen sufficiently large that the assumption:

$$\text{at } z = -l \text{ for all } t, \quad T_w = T_{w0}$$

introduces a negligible error into the final result.

Subject to these conditions, eqns. (37)–(39) may be solved by a finite difference method, originated by Murray and Landis [30], to yield the temperature distribution in the ice and water, the thickness of the ice layer and the heat flux to the liquid cryogen. In cases where the cryogenic liquid is a mixture, account must also be taken of the fact that  $T_B$  is a function of time. But in most cases the change of  $T_B$  with time, which must of course be determined by the independent mass and energy balance, is slow and can be easily incorporated into the numerical algorithm. In practice the algorithm requires an initial value for the thickness of the ice layer, but this can be set

at an arbitrarily small value, which is tantamount to the absence of any ice. If there is no significant ice layer growth from this initial value it may be assumed that a coherent ice layer is not formed and the analysis then also refers to the case of boiling on water.

**Heat transfer in confined spills**

Taken together the models described above provide a complete closed set of equations for the boiling of a cryogenic liquid on water. The empirical parameters of the models are the effective coefficients of thermal conductivity in the various fluid phases, which may be presumed to include some convective contributions and to therefore differ from the true thermal conductivity coefficients of Fourier's Law.

In order to demonstrate that the model presented above allows a satisfactory description of the boiling of cryogenic liquids on water we have performed calculations of heat fluxes for several confined spills.

First we have simulated the case of a confined spillage of 10.8 kg/m<sup>2</sup> of a liquid mixture of 90% methane and 10% ethane on a water surface of

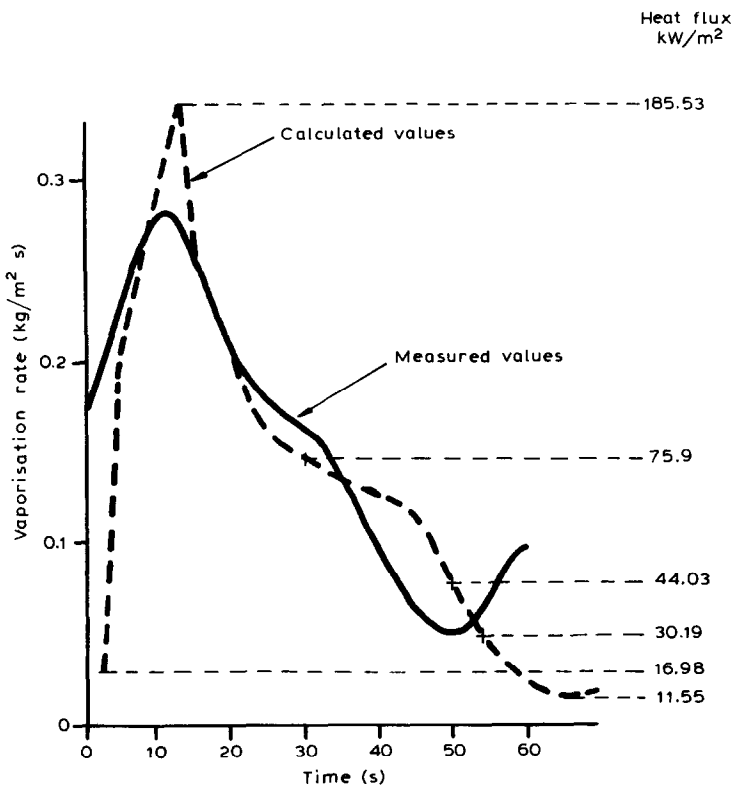


**Fig. 2.** Vaporisation rates for a confined spill of a methane/ethane mixture on water ; mixture composition: 90% methane, 10% ethane; spill quantity: 10.8 kg/m<sup>2</sup> on 143 cm<sup>2</sup> of water.

$1.43 \times 10^{-2} \text{ m}^2$  of water. These conditions correspond to those employed by Valencia-Chavez [9] in one of his experiments. In the simulation we have employed tabulated values of the thermophysical properties of the liquid mixture and water. In particular, the effective thermal conductivity of the water has been identified with the true thermal conductivity value. The results of the simulation are plotted in Fig. 2, in the form of plots of the mass flux of evaporated material; the predictions are directly compared with the experimental values. The agreement is good, all of the qualitative features of the experimental curve being reproduced by the simulation. The model predicts that the water surface freezes after about one second, in agreement with the rapid ice formation observed experimentally. The fall of the heat flux towards the end of the boil-off period corresponds to a rise in the bubble point of the liquid mixture accompanying the change in composition owing to the preferential evaporation of the more volatile component.

Figure 3 contains the results of simulations of other confined spills using a similar set of conditions in the form of plots of the heat flux. The spills considered are  $10 \text{ kg/m}^2$  of 90% methane and 10% ethane mixtures,  $30 \text{ kg/m}^2$  of the same mixture and  $10 \text{ kg/m}^2$  of almost pure ethane. For the larger spill, the heat flux reduces rapidly to about  $50 \text{ kW/m}^2$ . Subsequently, the changes are more gradual, associated with the growth in the ice layer, and a heat flux of about  $25 \text{ kW/m}^2$  is reached within 4 minutes.

The heat transfer model proposed for boiling of cryogenics on water is capable of describing many other experimental observations for confined spillages and seems able to describe the limited quantitative observations in unconfined spillages by adjustment of just one parameter as described

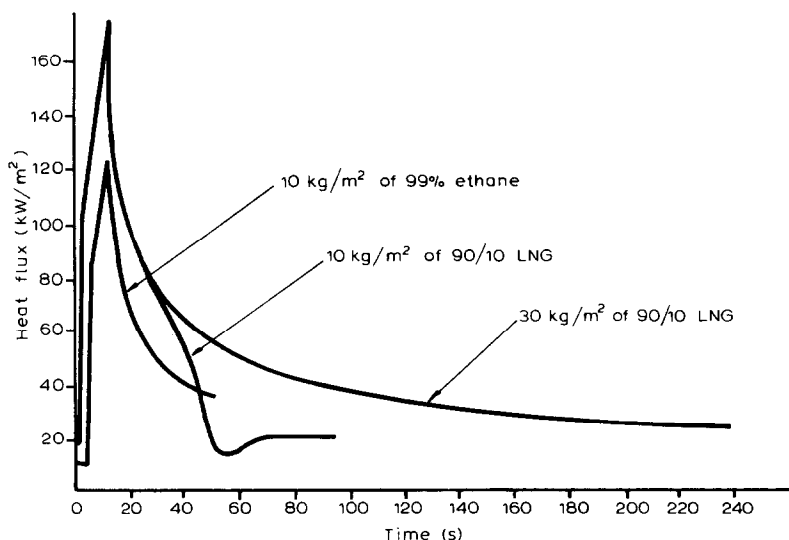


Fig. 3. Calculated heat fluxes for confined spills of LNG on water.

below. Thus, if a few carefully controlled experiments could be carried out on unconfined spillages, the present model would provide a sound basis for their interpretation. In addition, it makes possible the evaluation of the effective thermal conductivity of the water, which can be used to predict the heat fluxes to spills other than those investigated.

### Heat transfer and pool spreading in unconfined spills

Calculations have also been carried out for unconfined spills, but in this case a value for the effective (or eddy) thermal conductivity of water 10 times its molecular value was employed. This represented the general increase by an order of magnitude when passing from laminar to turbulent eddy diffusion. It was found that the water surface did not freeze for a considerable time despite the fact that film collapse occurred. This is explained by the high rate of heat transfer from the water to the interface. No significant amount of ice formation was found even after a prolonged period, in agreement with experimental observations of unconfined spills. Heat fluxes typical of film boiling were predicted.

Unconfined spills reported in the literature were simulated using the pool spread and vaporisation model derived above. Since the heat transfer model indicates that film boiling dominates in unconfined spills a typical film boiling heat flux of  $25 \text{ kW/m}^2$  was assumed. For comparison, a heat flux of  $100 \text{ kW/m}^2$ , often used in LNG spill simulations, was also assumed, as there was insufficient experimental evidence to evaluate the heat flux.

A 163-kg LNG spill conducted by the US Bureau of Mines (Burgess et al., [10]) was found to be better predicted using the film-boiling heat transfer rate (Fig. 4). A 38-kg LNG spill conducted by Shell (Boyle and Kneebone,

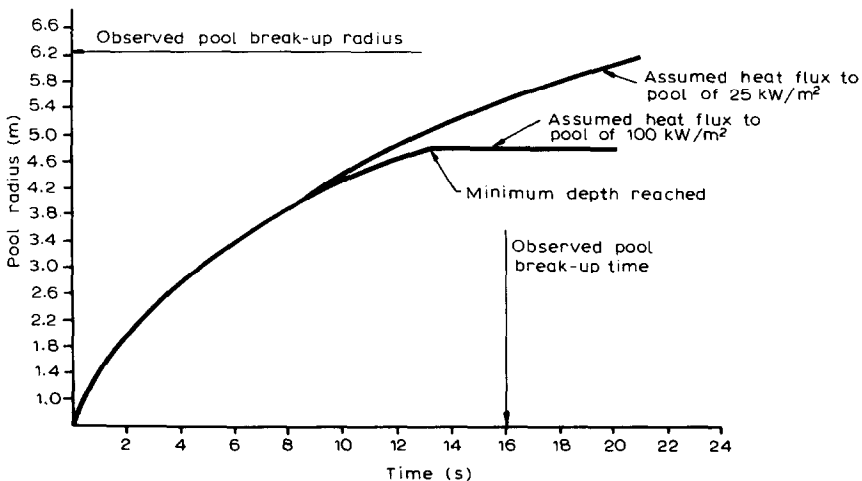


Fig. 4. Simulation of 163-kg spill of LNG on water (U.S. Bureau of Mines test).

[11]) was also found to be better predicted using the film-boiling heat transfer rate (Fig. 5); however, both simulations show the model to be in error on pool radius. Indeed, the Shell workers reported heat fluxes typical of film boiling in their unconfined spills. This provides some experimental confirmation for the above heat transfer model and a heat flux of  $25 \text{ kW/m}^2$ . However, theory strongly suggests this value.

A series of large LNG spills conducted by Esso (Feldbauer et al., [8]) were difficult to simulate because the LNG was sprayed onto the water, and considerable vaporisation undoubtedly occurred before the LNG contacted the water. A modelling of heat transfer to the spray jet is beyond the scope of this paper, so the simulation of these spills is not reported.

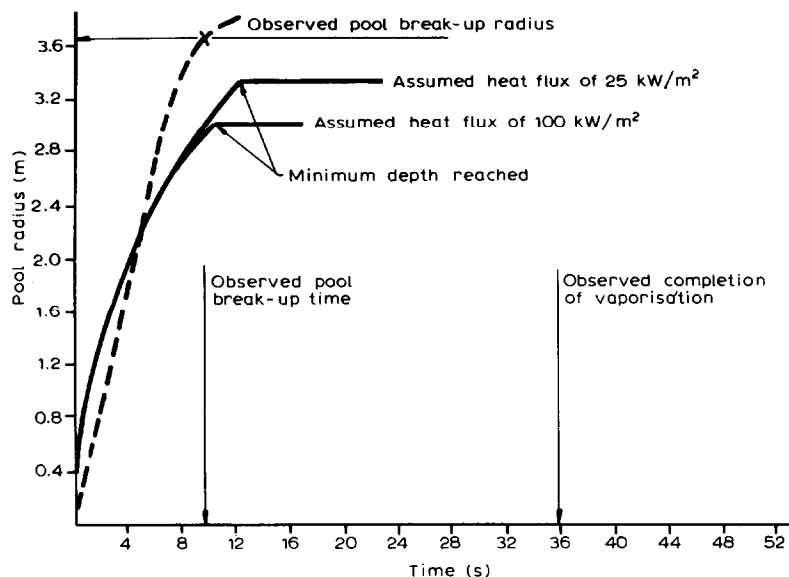


Fig. 5. Simulation of 38.1-kg spill of LNG on water (Shell test); — : model predictions; - - - : observed behaviour.

## Conclusion

A model of the spread and vaporisation of LNG has been described and tested against experimental results of small confined and unconfined spills of LNG. A major finding of this study is that heat transfer rates to LNG spreading on unconfined (turbulent) water are typical of film boiling rates. The simulation of LNG spills on unconfined water in hazard studies should therefore incorporate film-boiling heat transfer rates to the spreading pool. A value of  $25 \text{ kW/m}^2$  is a typical figure.

## List of symbols

### *Symbols*

$C_p$	Heat capacity.
$g$	Acceleration due to gravity.
$G_m$	Molar vaporisation rate.
$h$	Latent heat with two suffices denoting phase change.
$h$	Pool thickness (no suffices).
$i$	Enthalpy.
$k, K$	Constants.
$K_A, K_B$	Functions of pool temperature and composition.
$k_w$	Thermal diffusivity of water.
$l$	Depth in water where temperature is constant.
$L$	Length scale of an oil spill.
$L_m$	Molar liquid spill rate.
$L_{wi}$	Latent heat of fusion of ice.
$M$	Pool mass, $M_0$ initially.
$M_s, M_v$	Mass spilled; mass vaporised.
$q$	Heat flux to cryogenic liquid.
$r$	Radial co-ordinate.
$R, R^*$	Radius of pool.
$t$	Time.
$T$	Temperature.
$U$	Velocity.
$W_m$	Number of moles of material in the pool.
$x_A$	Molar methane portion of liquid pool ( $x_B$ , ethane).
$x_{AS}$	Molar methane portion of spilling liquid.
$y_A$	Molar methane portion of vapour ( $y_B$ , ethane).
$z$	Vertical coordinate.
$\delta$	Vapour layer thickness.
$\Delta T$	Temperature difference.
$\epsilon$	Ice layer thickness.
$\theta$	Temperature relative to freezing point of water.
$\lambda$	Effective thermal conductivity.
$\mu$	Viscosity.
$\rho$	Density.
$\sigma$	Surface tension.
$\phi$	Heat flux to liquid pool = $q$ .
<i>Suffices</i>	
A	Average (or methane fraction with $x, y$ ).
B	Boiling point of cryogen (or ethane fraction with $x, y$ ).
fc	Film collapse.
fg	Liquid to vapour phase change.

F	Freezing of water.
i	Ice.
l, L	Liquid.
lv	Liquid to vapour phase change.
LE	Leading edge.
m	Molar.
O	Initial.
o	Oil.
p	Pool.
s	Spilling liquid.
v	Vapour.
w	Water.

## References

- 1 J.A. Fay, The spread of oil slicks on a calm sea, in: D.P. Hoult (Ed.), *Oil on the Sea*, Plenum, New York, 1969, pp. 53–65.
- 2 T.K. Fannelop and G.D. Waldman, The dynamics of oil slicks or creeping crude, Amer. Inst. Aeronautics and Astronautics, NY, January 1971, Paper No. 71-14.
- 3 T.K. Fannelop and G.D. Waldman, Dynamics of oil slicks, *AIAA J.*, 10 (4) (1972) 506–510.
- 4 P.K.P. Raj and A.S. Kalelkar, Fire hazard presented by a spreading burning pool of liquefied natural gas on water, paper presented at the Combustion Inst. (USA) Western Section Meeting, El Segundo, CA, Fall 1973.
- 5 P.K.P. Raj and A.S. Kalelkar, Assessment models in support of the hazard assessment handbook, US Coastguard Report No CG-D-65-74, January 1974.
- 6 D.N. Gideon, A.A. Putnam and A.R. Duffy, Comparison of dispersion from LNG spills over land and water, Final Report for the American Gas Association, Project IS-3-7, September 1974.
- 7 W.G. May and P. Perumal, The spreading and evaporation of LNG on water, contributed paper, ASME Annual Winter Meeting, New York, November 1974.
- 8 G.F. Feldbauer, J.H. Heigl, W. McQueen, R.H. Whipp and W.G. May, Spills of LNG on water -- vaporization and downwind drift of combustible mixtures, Esso Research and Engineering, Report No. EE61E-72, May 1972.
- 9 J.A. Valencia-Chavez, The effect of composition on the boiling rates of liquefied natural gas for confined spills on water, D.Sc. Thesis, Massachusetts Institute of Technology, February 1978.
- 10 D.S. Burgess, J.N. Murphy and M.G. Zabetakis, Hazards of LNG spillage in marine transportation, US Department of Interior, Bureau of Mines, SRS Report No S4105, February 1970.
- 11 G.J. Boyle and A. Kneebone, Laboratory investigations into the characteristics of LNG spills on water. Evaporation, spreading and vapour dispersion, Shell Research Ltd, Thornton Research Centre, Chester, England, Report 6-32, March 1973.
- 12 E.M. Drake, A.A. Jeje and R.C. Reid, Transient boiling of liquefied cryogenes on a water surface. I. Nitrogen, methane and ethane, *Int. J. Heat Mass Transfer*, 18 (12) (1975) 1361–1368.
- 13 A.K. Dincer, E.M. Drake and R.C. Reid, Boiling of liquid nitrogen and methane on water, the effect of initial temperature, *Int. J. Heat Mass Transfer*, 20 (1977) 176–177.
- 14 D.P. Hoult, Oil spreading on the sea, *Ann. Rev. Fluid Mech.*, 4 (1972) 341–368.
- 15 J.A. Fay, Unusual fire hazard of LNG tanker spills, *Combust. Sci. Technol.*, F(2) (1973) 47–49.

- 16 G. Opschoor, Investigations into the spreading and evaporation of LNG spilled on water, *Cryogenics*, 17 (11) (1977) 629–633.
- 17 J.S. Turner, The coupled turbulent transports of salt and heat across a sharp density interface, *Int. J. Heat Mass Transfer*, 8 (1965) 759–767.
- 18 G. Opschoor, The spreading and evaporation of LNG and burning LNG spills on water, *J. Hazardous Materials*, 3 (1980) 249–266.
- 19 C.D. Lind, Explosion hazards associated with spills of large quantities of hazardous materials. Phase I, NTIS AD A00124/7GA, 1974.
- 20 B. Otterman, Analysis of large LNG spills on water, Part 1: Liquid spread and evaporation, *Cryogenics*, 15(8) (1975) 455–460.
- 21 P. Shaw and F. Briscoe, Evaporation from spills of hazardous liquids on land and water, SRD Report No R100 and presented at 5th Int Symp. on Transport of Dangerous Goods by Sea and Inland Waterways, Hamburg, April 1978.
- 22 W. Stein, Spreading and differential boil-off for a spill of liquefied natural gas on a water surface, in: Lawrence Livermore Laboratory Report UCID-17891, revision 1 December, 1978.
- 23 P.K.P. Raj, Models for cryogenic liquid spill behaviour on land and water, *J. Hazardous Materials*, 5 (1981) 111–130.
- 24 D.R. Blackmore, J.A. Eyre and G.G. Summers, Dispersion and combustion behaviour of gas clouds resulting from large spillages of LNG and LPG on to the sea, *Trans. Inst. Mar. Eng. (TM)*, 94 (1982) paper 29.
- 25 H.S. Carslaw and J.C. Jaeger, *Conduction of Heat in Solids*, 2nd edn., Oxford University Press, Oxford, 1959.
- 26 L.S. Sterman, Theory of heat transfer in boiling liquids, *Zh. Tekh. Fiz.*, 23 (2) (1953) 341–351.
- 27 S.S. Kutateladze, Hydrodynamic theory of changes in boiling processes under free convection, *Izv. Akad. Nauk SSSR, Otd. Tekh. Nauk*, 4 (1958) 529–536.
- 28 J.R. Moisis and P. Berenson, Hydrodynamic transition to nucleate boiling, *J. Heat Transfer*, 85c (3) (1963) 221–234.
- 29 Y.Y. Hsu and R.W. Graham, *Transport Processes in Boiling and Two-phase Systems*, McGraw-Hill, New York, 1976.
- 30 W.D. Murray and F. Landis, Numerical and machine solutions of transient heat conduction problems involving melting or freezing. Part I, *J. Heat Transfer*, 81 (1959) 106–120.
- 31 N. Zuber, On the stability of boiling heat transfer, *ASME Trans.*, 80 (1958) 711–720.